Synthesis of magneto-plasmonic hybrid material for cancer hyperthermia

Dinh Quang Thanh[1], Dinh Van Tuan[2], Nguyen Hoai Nam[3],
Nguyen Tien Anh[4], Nguyen Truong Xuan[3], Nguyen Luong Lam[1],
Dinh Thi Mai Thanh[1], Pham Hong Nam[3*], Nguyen Van Quynh[1*]

[1]University of Science and Technology of Hanoi (USTH), Vietnam Academy of Science and Technology;
[2]Electric Power University;
[3]Institute of Material Sciences (IMS), Vietnam Academy of Science and Technology;
[4]Department of Physics, Le Quy Don Technical University.
[*]Corresponding author: nguyen-van.quynh@usth.edu.vn; namph.ims@gmail.com.
Received 10 June 2022; Revised 28 July 2022; Accepted 10 August 2022; Published 26 August 2022.
DOI: https://doi.org/10.54939/1859-1043.j.mst.81.2022.128-137

ABSTRACT

Magnetic nanoparticle $CoFe_2O_4$-based hyperthermia is a promising non-invasive approach for cancer therapy. However, $CoFe_2O_4$ nanoparticles (NPs) have a low heat transfer efficiency, which limits their practical clinical applications. Hence, it is necessary to investigate the higher-performance magnetic NPs-based hybrid nanostructures to enhance their magnetic hyperthermia efficiency. This work presents a facile in situ approach for synthesizing cobalt ferrite ($CoFe_2O_4$) silver (Ag) hybrid NPs as optical-magnetic hyperthermia heat mediators. The prepared cobalt ferrite silver hybrid NPs exhibit a higher heat generation than that of individual Ag or $CoFe_2O_4$ NPs under simultaneous exposure to an alternating current magnetic field and laser source. The obtained results confirm that the hybridization of $CoFe_2O_4$ and Ag NPs could significantly enhance the hyperthermia efficiency of the prepared NPs. Therefore, the $CoFe_2O_4$-Ag hybrid NPs are considered as potential candidates for a high-performance hyperthermia mediator based on a simple and effective synthesis approach.

Keywords: Cobalt ferrite; Silver; Hybrid nanoparticles; Hyperthermia; Magnetic nanoparticles; Cancer treatment.

1. INTRODUCTION

Magnetic-optical nanomaterials are attracting much attention in biomedical research. The simultaneous activation of magnetic and optical properties allows magneto-optical composite nanomaterials to be used in cancer thermotherapy, imaging, and drug transmission [1]. The principle of thermotherapy in treating cancer is based on the heat-generating ability of the nanoparticles under the impact of external induced sources, such as magnetic field, laser, and infrared irradiation [2]. The localized temperature in the cancerous tumor area aims to reach the range of 42-46 °C to maximize effectiveness in killing cancer cells and avoid the influence on healthy cells.

Magnetic nanomaterials such as metal oxides (manganite) or ferrite (MFe_2O_4, M = Fe, Co, Zn, Mn) are full of interest for biomedical applications due to their high biological compatibility, less toxic, chemically stable, and simple fabrication method [3]. However, such individual materials have a relatively low saturation magnetization. So it requires a high particle concentration for achieving a sufficient temperature to treat cancer cells. A high amount of metal particles is toxic to healthy cells, this causes limitations in using heated particles for cancer therapy applications. To overcome this problem, several approaches have been proposed to fabricate a hybrid material that has magnetic nanoparticles in the size region, reaching the highest loss power value, hard-magnetic two-phase combination [4, 5]. This hybrid material has a high value of saturation magnetization and high magnetic resistance. It exhibits an excellent conversion efficiency of a magnetic particle to a heated particle. Therefore, even hybrid nanoparticles at low concentrations (ie. within biomedical limits) are enough to induce sufficient

heat to kill cancer cells. Another approach is to increase the intensity and frequency of the stimulating magnetic field; However, this approach is uneconomical and it produces various undesirable side effects while the body is exposed to high magnetic fields for long periods.

Noble metallic silver (Ag) NPs have been recognized as a potential anti-cancer or antibacterial agent and extensively studied in biomedical applications [6]. Recently, several recent studies have reported that Ag NPs combined with Fe_3O_4 NPs enhanced hyperthermia efficiency [7, 8]. However, Fe_3O_4 NPs generate heat which transmits a concise range and induces highly focused heating [9]. Hence the sensitivity of Ag NPs to Fe_3O_4 NPs-mediated hyperthermia may be limited by the separation of Fe_3O_4 and Ag NPs.

A judicious approach is to create a hybrid material of magnetic-optical components to overcome the disadvantages of using each material (magnetic or optical) separately, which allows a simultaneous combination of both magnetic heat generation and photo-induction heat generation. When optical and magnetic properties are integrated into a hybrid material, they exhibit not only some inherent advantages of each component but also novel physical properties created by the interactions between the two materials. Epinosa et al. combined both optical and magnetic effects to heat iron nanoparticles of Fe_3O_4 cubes and obtained SLP values of samples up to 5000 W/g, 2-15 times more than that of inducing by using magnetic fields only [7]. Abdulla-Al-Mamum et al. investigated the ability to kill cancer cells (ie. Hela cell) by using Fe_3O_4@Au hybrid NPs with a core/shell structure. The obtained results proved that by simultaneously stimulating (i.e magnetic field and the laser) of Fe_3O_4@Au particles with a concentration of 100 μg/mL, 100% of cancer cells were destroyed after only 5 minutes. The killing efficiency of cancer cells was two times higher when compared with using the magnetic field alone for heating [8].

One of the significant concerns to applying the magnetic particles in the biomedical field is their agglomeration in biological environments due to Van der Waals forces, high surface energy, and attractive magnetic forces existing among the particles. To prevent this agglomeration issue, the coating of nanoparticles with various agents serves as a solution that not only improved the stability of particles but also adds more specific functionality to prepared materials. Stabilization improved by the coating layer was achieved by an increase of surface charge (electrostatic forces) and by steric repulsion. Generally, it is more challenging to ensure the stability of water-based suspensions than suspensions in non-polar media, and so much lower contents of magnetic nanoparticles can be suspended. Usually, electrostatic repulsive forces between the nanoparticles related to a high electric surface charge are used to provide long-term stability. The surface charge is controlled simply by changing the pH value of the suspension [5, 7] or by the absorption of various polar molecules on the nanoparticles' surfaces. Adding surfactant simultaneously induces steric repulsive forces. Typically, the surfactant molecules are water-soluble and have more than one functional group; with at least one functional group they attach themselves to the nanoparticle surface, while the other functional groups ensure the hydrophilic nature of the nanoparticles. Different polar molecules have been used in water-based magnetic fluid, including amino acid [10], peptides [11], and also citric acid (CA). CA has three carboxyl groups and one hydroxyl group which assisted the chemical absorption into the magnetic nanoparticles by forming a carboxylate complex with the surface metal ions. In brief, CA has been considered as a good candidate to stabilize the colloidal cobalt ferrite silver NPs [12].

This work aims to optimize conditions for synthesizing $CoFe_2O_4$-Ag hybrid materials with high-performance hyperthermia and improved stability in the aqueous medium. The cobalt ferrite silver hybrid NPs with core-satellite structures exhibits a higher heat generation than the individual Ag or $CoFe_2O_4$ NPs with the combined exposure to an alternating current magnetic field and laser source. The hybridization of $CoFe_2O_4$ and Ag NPs shows a significant

enhancement of the hyperthermia efficiency of $CoFe_2O_4$ NPs. It allows for diverse applications in multidiscipline fields.

2. MATERIALS AND METHODS

2.1. Chemicals and synthesis of materials

The chemicals used to synthesize samples such as Citric acid monohydrate ($C_6H_8O_7.H_2O$, ≥ 99.5%); Silver (I) nitrate ($AgNO_3$, ≥ 99.5%); Acid nitric (HNO_3, ≥ 65%); Sodium hydroxide (NaOH, ≥ 98%); Absolute ethanol (C_2H_5OH, ≥ 95%) are commercial products which were purchased from Xilong Scientific Co., Ltd.

2.2. Experiment preparation

2.2.1. Cobalt ferrite ($CoFe_2O_4$) nanoparticles

Cobalt ferrite ($CoFe_2O_4$) nanoparticles were prepared by our colleague at Institute of Materials Science (IMS – VAST) from high purity chemicals purchased from Merck (Germany) including $FeCl_3.6H_2O$ (99.99%), $CoCl_2.6H2O$ (99.99%), and solid NaOH (99.99%); HCl. Solvents such as acetone and alcohol were purchased from Xilong Scientific Co., Ltd with 98.9% cleanliness.

The sample synthesis process is shown in figure 1 as follows: initially, $FeCl_3$ and $CoCl_2$ salts were mixed in a hydrochloric acid solution. A 2 ml of Co^{2+} solution was stirred vigorously with 4 ml of Fe^{3+} 1 M using a magnetic bar for 30 minutes. After that, the above mixture was added to 60 ml of NaOH 1M solution. The pH of the solution was then adjusted to pH = 11. All the solutions were put into an autoclave with a capacity of 80 ml. The autoclave was placed in the oven and heated from room temperature to 180 °C. After 2 hours, the autoclave was cooled to room temperature, and the product was separated from the solution and washed with distilled water and acetone. Finally, $CoFe_2O_4$ nanoparticles were obtained.

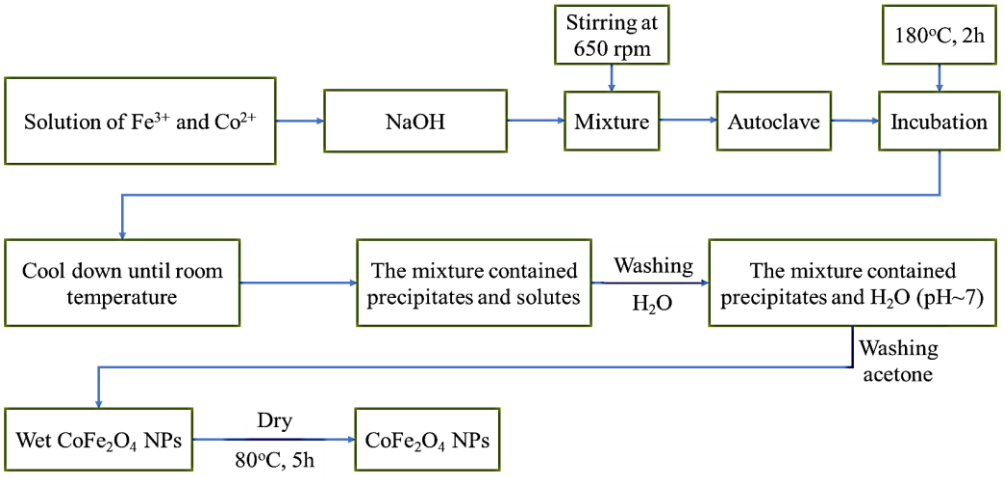

Figure 1. *The process of synthesizing $CoFe_2O_4$ nanoparticles.*

2.2.2. Chemicals to synthesize the hybrid $CoFe_2O_4$ – Ag NPs

Dispersion of MPs in distilled water by citric acid (Citric acid - coating on MPs):

Citrate-coated $CoFe_2O_4$ magnetic particles were prepared according to the procedure reported elsewhere [12]. Briefly, 10 mg of $CoFe_2O_4$ nanoparticles were dispersed in 50 ml of the aqueous solution of citric acid 0.07 M. The mixture is stirred at 700 rpm and 60 °C. After 90 min, allowing for the adsorption of the citric acid, the mixture was cooled down to room temperature. The nanoparticles were then suspended simply by adjusting the pH value of the mixture to 11. The pH of the mixture was adjusted by using the solutions of NaOH and HNO_3.

2.2.3. Synthesis of the hybrid nanoparticles $CoFe_2O_4$ – Ag

Figure 2 shows the process of synthesizing $CoFe_2O_4$ – Ag.

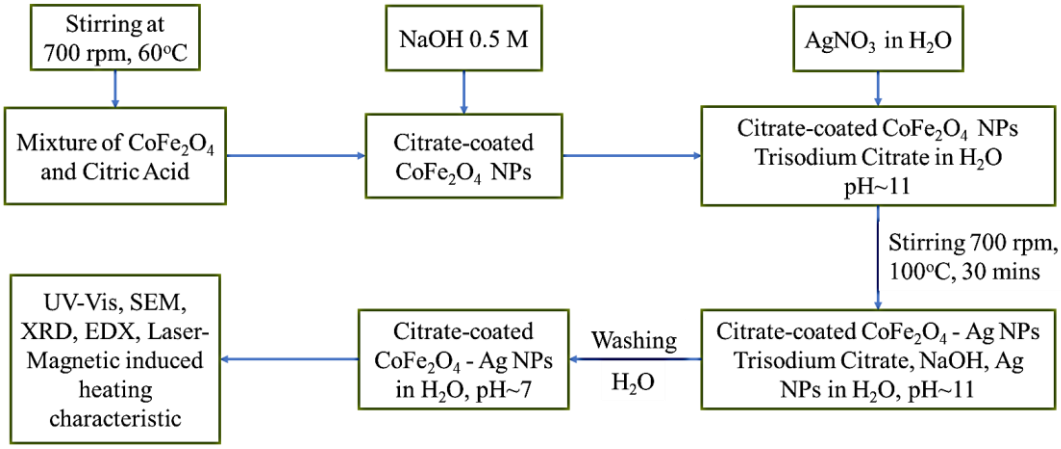

Figure 2. *The process of synthesizing $CoFe_2O_4$ – Ag.*

The mixture prepared above was heated up to the boiling temperature. When the mixture was boiled, a certain amount of silver nitrate was added to the mixture. The reaction was carried out in dark. After vigorous stirring of the mixture for 30 minutes to ensure silver ions reacted completely with citrate ions, the mixture was cooled down to room temperature. Finally, the prepared $CoFe_2O_4$-Ag NPs were obtained and washed thoroughly several times with distilled water under an external magnetic field applied until the remaining solution was clear.

Two different samples of hybrid NPs were synthesized by changing the weight ratio of silver nitrate and $CoFe_2O_4$ NPs (1:2 and 1:5). The amount of $CoFe_2O_4$ NPs was fixed to 10 mg. Table 1 describes the synthesis conditions of the hybrid NPs.

Table 1. *Conditions of the preparation of the hybrid NPs.*

Sample	**V**	**t**	**pH**	**[CA]**	**[Ag^+]**	**[$CoFe_2O_4$]**	**w**	**Reaction duration**	**Stirring**
	ml	°C		mM	mM	mg/ml		minutes	rpm
T1	50	100	10.94	7	1	0.2	1:2	30	700
T2	50	100	11.02	7	0.4	0.2	1:5	30	700

Note: w – The weight ratio of Ag and $CoFe_2O_4$; V – The volume of the mixture; t – The temperature of the reaction.

Ag NPs were synthesized in a similar procedure to $CoFe_2O_4$ – Ag NPs however $CoFe_2O_4$ was absent in the reaction. The free Ag nanoparticles were washed similarly to the $CoFe_2O_4$ - Ag NPs, but during the washing process, a centrifuge was used to collect the seeds instead.

2.3. Characterization techniques

2.3.1. UV-Vis

UV-Vis molecular absorption spectroscopy (Ultra Violet - Visible) is used to study the interaction of a material with the illuminated light to examine the optical properties of a material. As a result, the effective excitation wavelength can be determined for each material. Since the optical properties of the solution containing the ferromagnetic - noble metal hybrid nanoparticles (Ag, Au) depend on the shape, size, and concentration of the material, the UV-Vis molecules absorption spectroscopy method can be used to determine the above properties.

UV-Vis spectra were recorded on the Shimadzu UV-1280 spectrometer (Japan) at the Advanced Materials and Applications Laboratory (AMA Lab) -USTH.

2.3.2. Scanning electron microscopy (SEM)

Scanning electron microscopy (SEM) was used to characterize surface morphologies. SEM measurements and analyses were performed on scanning electron microscopy equipment HITACHI S-4800 at IMS - VAST. The highest magnification can reach 800,000 times; the resolution can reach 2 nm at a voltage of 1 kV.

2.3.3. Laser-magnetic induced heating characterization

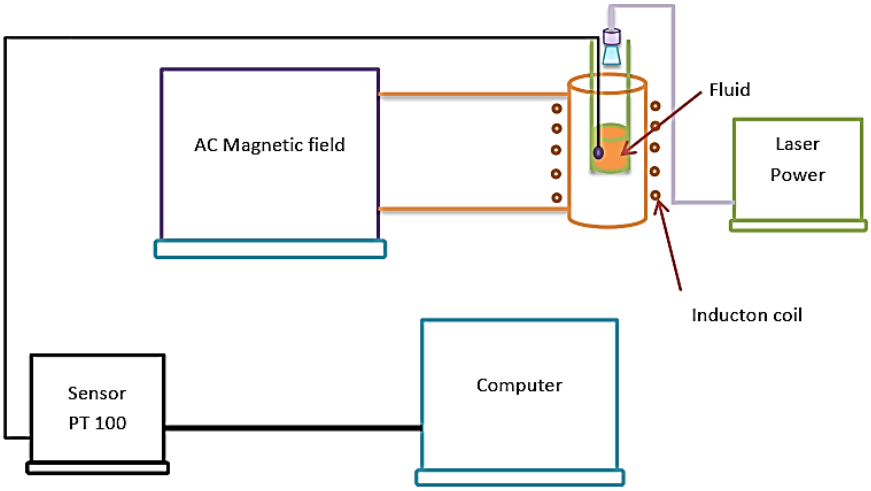

Figure 3. *Laser-magnetic induced heating experiment setup.*

This experiment designed illustrated in figure 3:

Magnetic field alternating system: Model UHF-20A, the capacity of 20 kW. The frequency varies in the range of 100 ÷ 500 kHz and the magnetic field strength is 45 ÷ 400 Oe generated by the induction coil (7 turns; inner diameters of 3 cm, 4 cm, 5 cm, and 6 cm; coil length of 11.5 cm). A laser system with a wavelength of 532 nm and power of 0 -2.5 W/cm^2 has been used as a stimulating source.

The prepared sample is dispersed in water and insulated from the outside by a glass bottle with a vacuum of 10-3 ÷ 10-4 Torr. The sample temperature was measured after activating the magnetic field and the laser source by a PT100 sensor with an accuracy of 0.5 ℃ in the range from 0 ℃ to 250 ℃ and connected to a computer to record data.

3. RESULTS AND DISCUSSION

3.1. Stabilization of $CoFe_2O_4$ NPs in an aqueous medium by citric acid

Figure 4 shows the effectiveness of citrate coating on $CoFe_2O_4$ NPs, in which the citrate-coated $CoFe_2O_4$ NPs are more stable than the uncoated NPs.

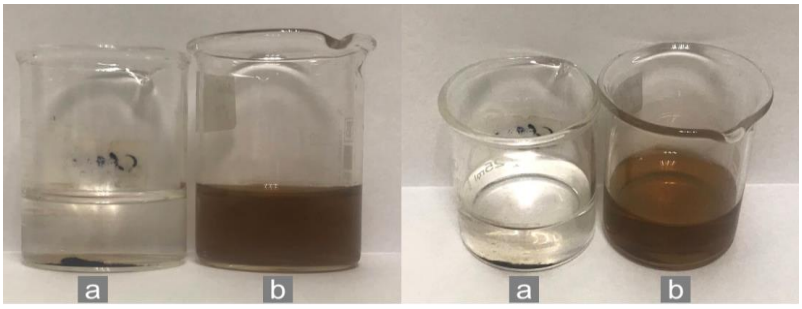

Figure 4. *$CoFe_2O_4$ NPs dispersed in an aqueous medium (a) without and (b) with citrate-coating after 5 minutes separating magnetically.*

As can be seen in figure 4, after separating magnetically, the uncoated $CoFe_2O_4$ NPs agglomerated to the bottom of the cup, and the solution remained was then transparent appearance. In contrast, the rate of agglomeration observed in a solution of the coated $CoFe_2O_4$ NPs decreased obviously. Consequently, the remained solution is brown, which indicates the presence of citrate-coated $CoFe_2O_4$ NPs decreases the agglomeration of nanoparticles. The mechanism of the stabilization of $CoFe_2O_4$ NPs by citric acid is due to chemisorb to the iron oxide nanoparticle by forming a carboxylate group with the Fe–OH molecules present on the NPs surface, leaving one or two carboxyl groups negatively charged. The repulsive force between the coated NPs enhances the stability of the particles in water [13, 14]. It can be concluded that citric acid stabilized the $CoFe_2O_4$ NPs for a desirable dispersion in an aqueous medium.

3.2. UV-Vis spectra

The optical properties of cobalt ferrite silver hybrid NPs were characterized using UV-Vis absorption spectra shown in Fig. 5 and Fig. 6

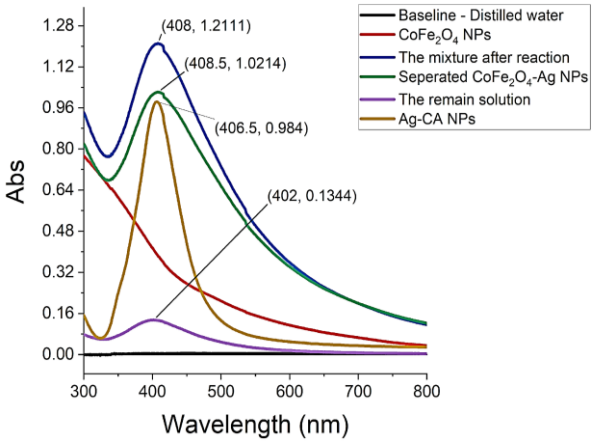

Figure 5. *UV-Vis spectra of the aqueous solution of Ag, $CoFe_2O_4$, and Ag - $CoFe_2O_4$ NPs.*

In Fig. 5, Ag NPs and $CoFe_2O_4$-Ag hybrid NPS samples show intense peaks located at 407 nm and 408 nm, respectively, which were attributed to the absorbed peak of Ag NPs due to the localized surface plasmon resonance (LSPR) phenomena. The LSPR peak of the mixture after the reaction implies that Ag NPs have been successfully formed by the reduction of Ag^+ to Ag^0 in the presence of citrate ions. Besides, after magnetically separating, the obtained NPs and the remained solution also have peaks at 408 and 402 nm, respectively. These peaks are similar to the ones observed in the initial mixture but with lower intensity. It proves that Ag NPs have partly deposited on the surface of the $CoFe_2O_4$ NPs while the remained NPs stay freely in the mixture.

To prove that the Ag NPs decorate to the $CoFe_2O_4$ NPs in the final product, the washing process of the sample T1 is examined by the UV-Vis method. The result was shown in figure 6. In each washing time, the mixture is magnetically separated into two parts: the part of solution contains free-AgNPs (Fig. 6a) and the separated $CoFe_2O_4$-Ag particles (Fig. 6b). The maximum absorbance wavelength of the remaining NPs tended to be red-shifted compared to that of the previous one, which is due to the local dielectric effect according to classical Mie theory [15]. Similar redshifts have also been reported before [15].

Furthermore, the LSPR wavelengths of the rest part solutions are around 408 nm, and the intensity of the peaks decreased after each washing, which implies that the free Ag NPs have been rinsed away from the hybrid NPs. At the 6^{th} cycle of washing, the LSPR peak disappears, which means most of the free Ag NPs are removed, and the hybrid NPs are clean. At this stage, there are only Ag NPs attached to the $CoFe_2O_4$ NPs.

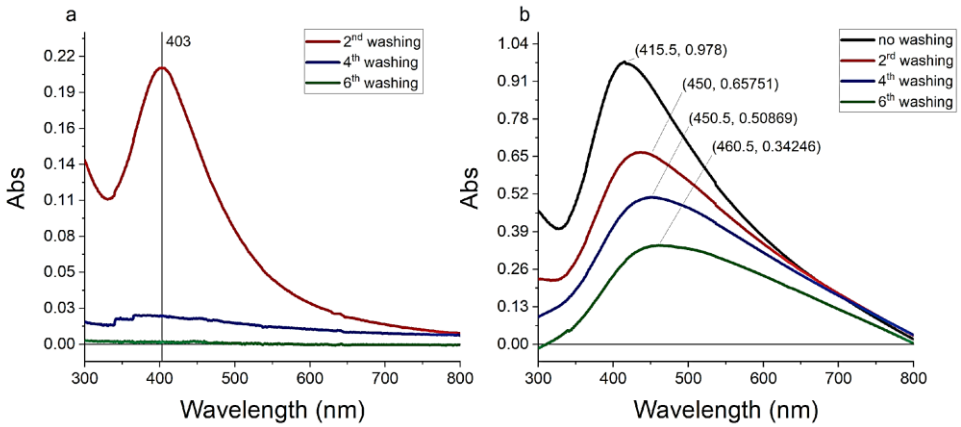

Figure 6. *UV-Vis spectra of solution contains free- AgNPs (a) and magnetically separated $CoFe_2O_4$-Ag nanoparticles (b) after the washing process.*

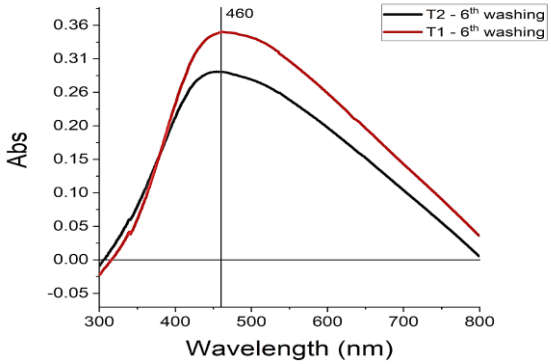

Figure 7. *UV-Vis spectra of the hybrid NPs of different ratios w after washing.*

In figure 7, the LSPR peaks locate at the same wavelength of 460 nm, which indicates the presence of Ag NPs in both samples. Furthermore, the LSPR peak of T1 gives a higher intensity than that of T2 (0.34662 and 0.28622, respectively), due to the amount of Ag NPs generated in T1 was higher than the one in T2. It demonstrated that the weight ratio of Ag and $CoFe_2O_4$ influences the formation of Ag NPs on the $CoFe_2O_4$ NPs.

3.3. SEM and EDX results

The SEM images of $CoFe_2O_4$ NPs and the prepared $CoFe_2O_4$-Ag NPs are presented in figure 8, and their average diameters are estimated to be 30 – 50 nm and 10 – 15 nm, respectively. The darker particles are $CoFe_2O_4$, while the brighter small particles are AgNPs because it is well-known that Ag NPs have higher conductivity than $CoFe_2O_4$ NPs.

Figure 8 indicates that compare to the $CoFe_2O_4$ NPs (Fig. 8a), Ag NPs were successfully aggregated on the $CoFe_2O_4$ NPs surface by the reduction of Ag^+ ions by citrate anions (Fig. 8b and Fig. 8c). It is obvious that many small Ag NPs were decorated on the $CoFe_2O_4$ NPs surface. However, the size of AgNPs is not homogeneous, the existence of a large AgNPs can be still observed. It can be explained that the generation of Ag seeds is speedy and strongly influence by the weight ratio of Ag and $CoFe_2O_4$. When the amount of $AgNO_3$ added is a ratio of 1:2, [17] the quantity of silver particles is sufficient for generating AgNPs with uniform sizes (Fig.8b). However, when amount of added Ag increased (weight ratio of Ag/$CoFe_2O_4$ is 1:5), some larger AgNPs were formed on the surface (Fig. 8c). It can be concluded that the amount of Ag NPs attached with $CoFe_2O_4$ NPs increased when increasing the weight ratio of Ag and $CoFe_2O_4$.

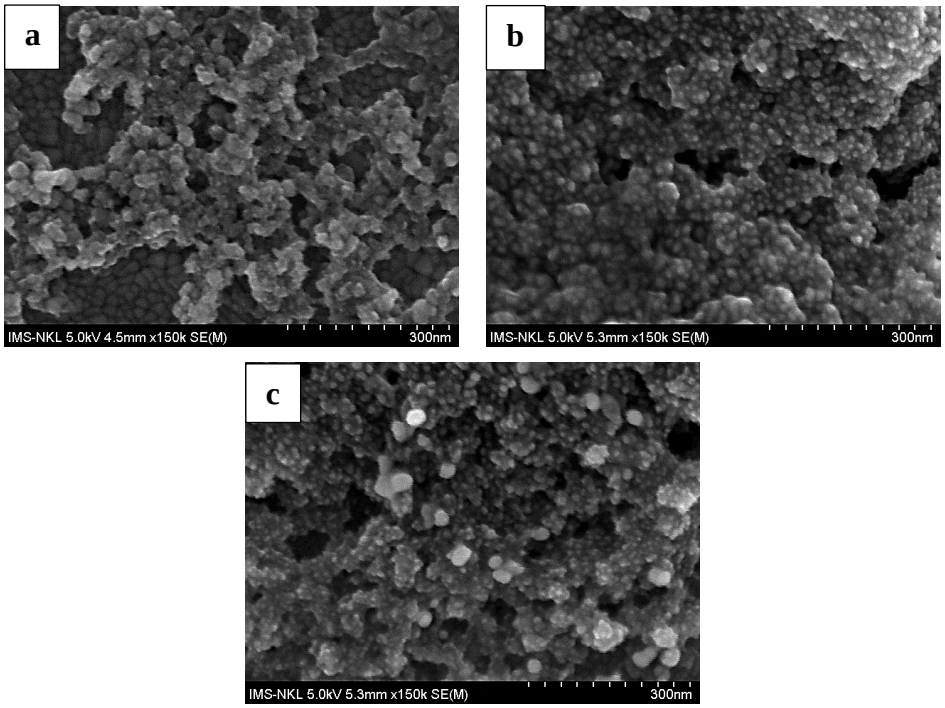

Figure 8. *SEM images of (a) $CoFe_2O_4$ NPs and (b) $CoFe_2O_4$-Ag hybrid NPs at 1:2 (sample T1) and (c) 1:5 (sample T2) weight ratios of Ag and $CoFe_2O_4$, respectively.*

The presence of Ag was confirmed with the EDX analysis of the samples T1 and T2, as illustrated in figure 9. While the $CoFe_2O_4$ NPs consisted of Co, Fe, and O elements, the hybrid Ag – $CoFe_2O_4$ NPs, which consisted of not only Co, Fe, and O but also Ag was observed. Besides the above elements, the result indicated the presence of Si, Na, and In which are the components of the ITO substrate. Moreover, the signal of Na was detected in the sample T1, which can be explained that Na was not entirely removed in the washing process.

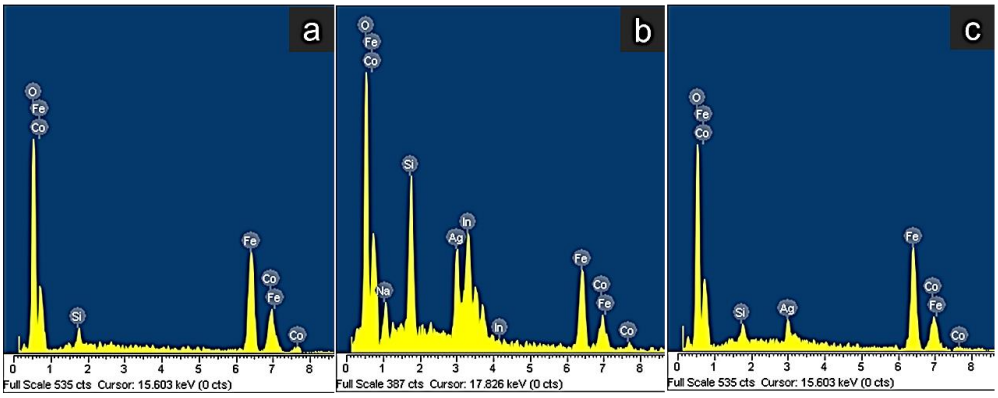

Figure 9. *EDX image of (a) $CoFe_2O_4$ NPs, (b) T1 and (c) T2.*

3.5. Laser-magnetically induced heating characteristics of $CoFe_2O_4$-Ag hybrid NPs

Figure 10 exhibits the induced heating characteristics of $CoFe_2O_4$-Ag hybrid NPs with w = 1:5. When applying a single source ACMF or laser, the temperature of the sample raised approximately 33 ^oC after 200 sec laser treatment and quickly reached the saturated temperature of 35 ^oC and 37 ^oC within 430 sec, respectively. It showed that the optical hyperthermia generated more heat than the magnetic hyperthermia but took much more time to reach a

saturated temperature. Furthermore, when laser and ACMF are applied simultaneously, the temperature increased dramatically. Specifically, in this case, within 200 s, the temperature increased around 36% and 30% compared to individual magnetic and laser-induced heating respectively. It demonstrated that the combination of the two stimulated sources induces heat faster compared to individual hyperthermia (optical or magnetic). These obtained results are in good agreement with the findings reported on Fe_3O_4 @ Au [18], and Fe_3O_4 @ Ag [19].

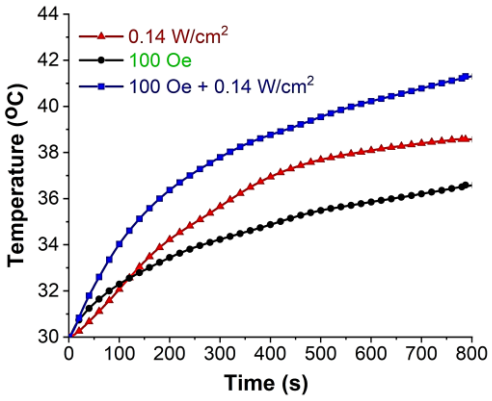

Figure 10. *Temperature-time curves of aqueous solutions of $CoFe_2O_4$-Ag with a concentration of 1 mg/mL; red – only laser applied, black – only ACMF applied, and blue – laser-ACMF applied.*

4. CONCLUSIONS

In this work, the hybrid cobalt ferrite silver NPs were successfully synthesized by the chemical approach. The prepared hybrid NPs have a high density and the average sizes vary from 10 to 50 nm in diameter. Significantly, by introducing Ag NPs to the core of magnetic NPs of $CoFe_2O_4$, the hyperthermia efficiency of $CoFe_2O_4$/AgNPs was greatly enhanced when applying laser source and AMFC simultaneously compared to an individual stimulation, which can be attributed to the combination of magnetically induced heating of $CoFe_2O_4$ and heat-assisting of Ag NPs. Therefore, the prepared hybrid NPs have great potential for the application of cancer hyperthermia.

Acknowledgment: *This work was funded by Vietnam Academy of Science and Technology (VAST) under grant number DL0000.06/20-22.*

REFERENCES

[1]. C.-H. Wu, J. Cook, S. Emelianov, and K. Sokolov, *"Multimodal Magneto-Plasmonic Nanoclusters for Biomedical Applications,"* Adv. Funct. Mater., vol. 24, no. 43, pp. 6862–6871, (2014).

[2]. J. Kolosnjaj-Tabi, I. Marangon, A. Nicolas-Boluda, A. K. A. Silva, and F. Gazeau, *"Nanoparticle-based hyperthermia, a local treatment modulating the tumor extracellular matrix,"* Pharmacol. Res., vol. 126, pp. 123–137, (2017).

[3]. C. S. S. R. Kumar and F. Mohammad, *"Magnetic nanomaterials for hyperthermia-based therapy and controlled drug delivery,"* Adv. Drug Deliv. Rev., vol. 63, no. 9, pp. 789–808, (2011).

[4]. P. H. Nam *et al.*, *"Polymer-coated cobalt ferrite nanoparticles: synthesis, characterization, and toxicity for hyperthermia applications,"* New J. Chem., vol. 42, no. 17, pp. 14530–14541, (2018).

[5]. J.-H. Lee *et al.*, *"Exchange-coupled magnetic nanoparticles for efficient heat induction,"* Nat. Nanotechnol., vol. 6, no. 7, pp. 418–422, (2011).

[6]. P. Kaur, M. L. Aliru, A. S. Chadha, A. Asea, and S. Krishnan, *"Hyperthermia using nanoparticles – Promises and pitfalls,"* Int. J. Hyperth., vol. 32, no. 1, pp. 76–88, (2016).

[7]. A. Espinosa, R. Di Corato, J. Kolosnjaj-Tabi, P. Flaud, T. Pellegrino, and C. Wilhelm, *"Duality of Iron Oxide Nanoparticles in Cancer Therapy: Amplification of Heating Efficiency by Magnetic Hyperthermia and Photothermal Bimodal Treatment,"* ACS Nano, vol. 10, no. 2, pp. 2436–2446, (2016).

[8]. M. Abdulla-Al-Mamun, Y. Kusumoto, T. Zannat, Y. Horie, and H. Manaka, *"Au-ultrathin functionalized core–shell (Fe3O4@Au) monodispersed nanocubes for a combination of magnetic/plasmonic photothermal cancer cell killing," RSC Adv.*, vol. 3, no. 21, p. 7816, (2013).
[9]. A. Riedinger *et al.*, *"Subnanometer Local Temperature Probing and Remotely Controlled Drug Release Based on Azo-Functionalized Iron Oxide Nanoparticles,"* Nano Lett., vol. 13, no. 6, pp. 2399–2406, (2013).
[10]. M. F. Zarabi, N. Arshadi, A. Farhangi, and A. Akbarzadeh, *"Preparation and Characterization of Gold Nanoparticles with Amino Acids, Examination of Their Stability,"* Indian J. Clin. Biochem., vol. 29, no. 3, pp. 306–314, (2014).
[11]. W.-Z. Shen, S. Cetinel, K. Sharma, E. R. Borujeny, and C. Montemagno, *"Peptide-functionalized iron oxide magnetic nanoparticle for gold mining,"* J. Nanoparticle Res., vol. 19, no. 2, p. 74, (2017).
[12]. M. E. de Sousa *et al.*, *"Stability and Relaxation Mechanisms of Citric Acid Coated Magnetite Nanoparticles for Magnetic Hyperthermia,"* J. Phys. Chem. C, vol. 117, no. 10, pp. 5436–5445, (2013).
[13]. *"Methods for Assessing Surface Cleanliness,"* in Developments in Surface Contamination and Cleaning, Volume 12, Elsevier, pp. 23–105, (2019).
[14]. S. Campelj, D. Makovec, and M. Drofenik, *"Preparation and properties of water-based magnetic fluids,"* J. Phys. Condens. Matter, vol. 20, no. 20, p. 204101, (2008).
[15]. Q. Ding *et al.*, *"Shape-controlled fabrication of magnetite silver hybrid nanoparticles with high performance magnetic hyperthermia,"* Biomaterials, vol. 124, pp. 35–46, (2017).
[16]. S. B. Waje, M. Hashim, W. D. W. Yusoff, and Z. Abbas, *"X-ray diffraction studies on crystallite size evolution of $CoFe_2O_4$ nanoparticles prepared using mechanical alloying and sintering,"* Appl. Surf. Sci., vol. 256, no. 10, pp. 3122–3127, (2010).
[17]. S. Peng, C. Lei, Y. Ren, R. E. Cook, and Y. Sun, *"Plasmonic/Magnetic Bifunctional Nanoparticles,"* Angew. Chemie Int. Ed., vol. 50, no. 14, pp. 3158–3163, (2011).
[18]. Espinosa A., R. Di Corato, J. Kolosnjaj-Tabi, P. Flaud, T. Pellegrino, and C. Wilhelm, *"Duality of iron oxide nanoparticles in cancer therapy: amplification of heating efficiency by magnetic hyperthermia and photothermal bimodal treatment"* ACS Nano, vol. 10, pp. 2436-2446, (2016).
[19]. Das R., N. Rinaldi-Montes, J. Alonso, Z. Amghouz, E. Garaio, J. A. Garcia, P. Gorria, J. A. Blanco, M.-H. Phan, and H. Srikanth, *"Boosted hyperthermia therapy by combined AC magnetic and photothermal exposures in Ag/Fe3O4 nanoflowers"* ACS Appl. Mater. Interfaces, vol. 8, pp. 25162-25169, (2016).

TÓM TẮT

Tổng hợp hệ vật liệu lai quang – từ định hướng cho ứng dụng nhiệt trị ung thư

Các hạt nano từ tính sinh nhiệt dựa trên nền vật liệu $CoFe_2O_4$ là vật liệu tiềm năng cho hướng tiếp cận điều trị ung thư không xâm lấn. Tuy vậy, các hạt nano từ tính $CoFe_2O_4$ thường cho hiệu suất truyền nhiệt thấp, đã hạn chế nhiều trong phát triển các ứng dụng y sinh trong thực tế. Do đó, việc nghiên cứu phát triển các hệ vật liệu lai trên nền vật liệu từ cho hiệu suất truyền nhiệt cao hơn là cần thiết. Nghiên cứu này tập trung phát triển phương pháp đơn giản để tổng hợp trực tiếp hệ vật liệu lai quang từ coban ferrit ($CoFe_2O_4$) và hạt nano bạc (AgNPs), cho các ứng dụng yêu cầu hiệu suất sinh và truyền nhiệt cao. Nghiên cứu chỉ ra rằng, vật liệu lai quang-từ đã tổng hợp cho hiệu suất sinh nhiệt lớn hơn so với các vật liệu đơn lẻ (hạt nano bạc) và hạt nano từ $CoFe_2O_4$ khi cùng được kích thích dưới một điều kiện là từ trường xoay chiều hay laze. Kết quả thu được chứng minh rằng việc lai hóa giữa hạt nano từ và hạt nano bạc đã cho hiệu suất sinh nhiệt vượt trội. Vì vậy, hệ vật liệu tổng hợp $CoFe_2O_4$- là vật liệu tiềm năng cho lĩnh vực y sinh, điều trị ung thư bằng phương pháp không xâm lấn.

Từ khoá: Coban ferit; Hạt nano bạc; Vật liệu lai hóa; Hiệu ứng sinh nhiệt; Hạt nano từ tính; Nhiệt trị ung thư.